J. Fluid Mech. (1991), *vol.* 226, *pp.* 565–571
Printed in Great Britain

The continuous spectrum of the Orr–Sommerfeld equation: note on a paper of Grosch & Salwen

By A. D. D. CRAIK

Department of Mathematical and Computational Sciences, University of St. Andrews, St. Andrews, Fife, KY16 9LN, UK

(Received 26 January 1990 and in revised form 24 November 1990)

Grosch & Salwen (1978) discuss the continuous-spectrum contribution in both temporal and spatial stability problems that are governed by the linear Orr–Sommerfeld equation. Their computed temporal continuum eigenfunctions for the Blasius boundary layer and for a laminar jet profile show surprising differences. This note provides an improved physical understanding of the results through a simple model, and shows that these differences are more apparent than real.

1. The Grosch-Salwen results

As part of their instructive examination of the continuous spectrum of the Orr–Sommerfeld equation, Grosch & Salwen (1978, hereinafter denoted as I) give results for temporally damped continuum modes associated with (*a*) the Blasius boundary-layer profile and (*b*) the jet profile $U(y) = 1-\tanh^2 y$. For ease of reference, some of these results are briefly described.

A single 'continuum mode' has a far-field structure, as $y \to \infty$ outside the shear-flow region, of (cf. I, equation (67))

$$\psi = \exp[\mathrm{i}\alpha(x-ky-ct)] + B\exp[\mathrm{i}\alpha(x+ky-ct)] + C\,\mathrm{e}^{-\alpha y}\exp[\mathrm{i}\alpha(x-ct)]. \tag{1}$$

Here, k is an arbitrary real constant, α is the streamwise wavenumber, αk a transverse wavenumber and R is the Reynolds number. The complex phase velocity c of such continuous-spectrum modes is

$$c = U_\infty - \mathrm{i}(1+k^2)\,\alpha/R \tag{2}$$

where U_∞ denotes the free-stream velocity ($U_\infty = 1$ for Blasius flow and 0 for the jet). The coefficient of the first exponential term is here normalized to unity and B, C are complex constants which must be determined by solving the homogeneous boundary-value problem posed by the Orr–Sommerfeld equation and the rigid-wall boundary conditions.

The first exponential in (1) may be thought of as representing an 'incoming' wave with wavenumber vector $(\alpha, -k\alpha)$ making an angle $-\theta$ with the x-axis, where

$$\theta = \tan^{-1} k. \tag{3}$$

The B-term is then an associated 'outgoing' wave and the C-term a 'trapped' or evanescent mode that decays as $y \to \infty$. However, there is no energy or momentum flux associated with the incoming and outgoing waves: they are passively convected by the free stream U_∞, while decaying exponentially by viscous dissipation.

Computational results of I show magnitudes and phases of B and C at specific chosen values of α and of R as the angle θ is allowed to vary from 0 to 90°: that is,

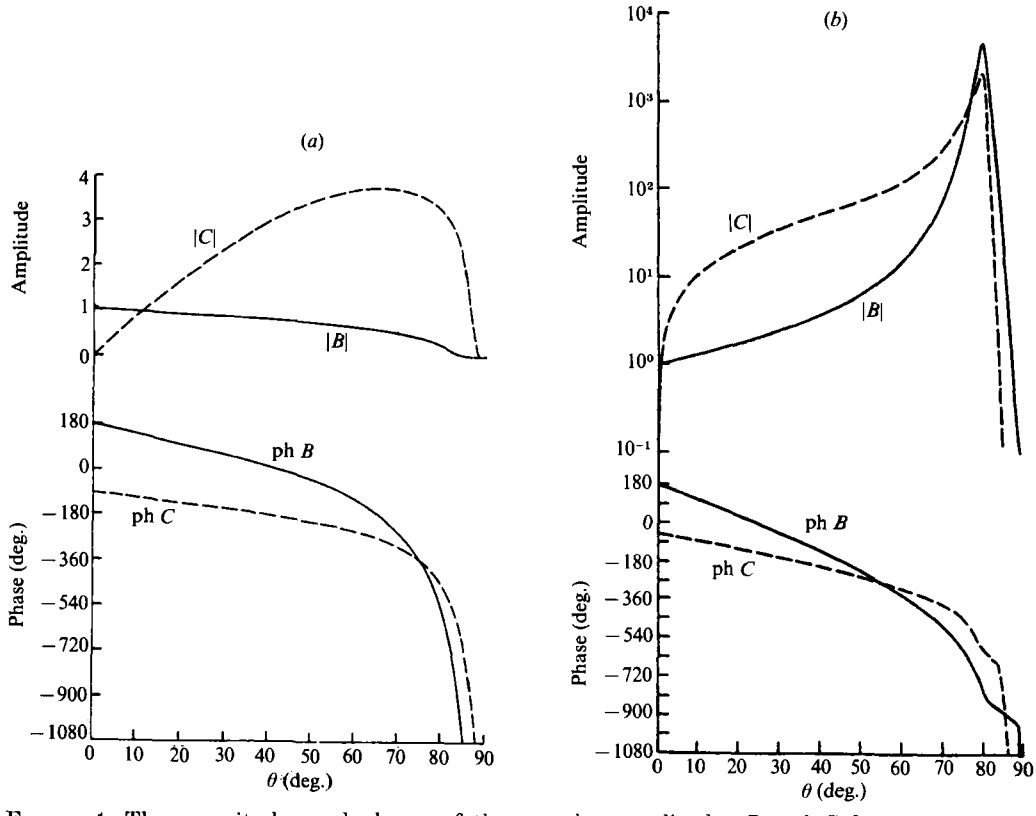

FIGURE 1. The magnitudes and phases of the complex amplitudes B and C for the temporal continuum modes, from Grosch & Salwen (1978): (*a*) for the Blasius boundary layer at $\alpha = 0.179$, $R = 580$; (*b*) for the two-dimensional laminar jet at $\alpha = 1$ and $R = 50$.

as k varies from 0 to infinity. Figures 2 and 3 of I are here reproduced in figure 1 (*a*, *b*): the curves of figure 1 (*a*) are for Blasius flow at $R = 580$ and $\alpha = 0.179$: while those of figure 1 (*b*) are for the jet profile with antisymmetric modes at $R = 50$ and $\alpha = 1.0$ (it is stated in I that results for symmetric modes are virtually indistinguishable from these).

As remarked in my monograph (Craik 1985, p. 54), these results are puzzling. In both cases, $|B| = 1$ and $C = 0$ at $\theta = 0$; but, as θ increases, $|B|$ gradually decreases towards zero in case (*a*) while it rapidly increases in case (*b*) to a maximum of 4850. Though $|C|$ increases in both figures as θ increases, the maximum value of $|C|$ is only 3.7 in (*a*) but 2300 in (*b*). These differences, and the curiously rapid phase variations at larger values of θ, have received no satisfactory explanation. Grosch & Salwen's own assertion (I, p. 48) that the difference in amplitudes 'was to be expected in view of the very low critical Reynolds number for a jet... as compared with... the Blasius boundary layer' is unjustified.

2. A simple model flow

Consider the piecewise-linear profile

$$\left.\begin{aligned} U &= 1 \quad (y > h), \\ U &= y/h \quad (0 < y < h) \end{aligned}\right\} \tag{4}$$

that is crudely representative of a boundary-layer flow. If we restrict attention meantime to inviscid cases ($R = \infty$), the appropriate forms for the disturbance in the two regions are

$$\psi = \begin{cases} \exp[\mathrm{i}\alpha(x-ky-t)] + B\exp[\mathrm{i}\alpha(x+ky-t)] + C\,\mathrm{e}^{-\alpha y}\exp\{\mathrm{i}\alpha(x-t)\} & (y > h) \\ D\sinh(\alpha y)\exp\{\mathrm{i}\alpha(x-t)\} & (0 < y < h), \end{cases} \tag{5}$$

the latter of which satisfies the inviscid boundary condition at the wall. To match ψ at $y = h$, we need

$$D\sinh(ah) = \mathrm{e}^{-\mathrm{i}\alpha kh} + B\,\mathrm{e}^{\mathrm{i}\alpha kh} + C\,\mathrm{e}^{-\alpha h}. \tag{6}$$

Also, continuity of pressure across the interface yields the condition

$$\left[-\frac{\partial p}{\partial x}\right]_-^+ = \left[\left(\frac{\partial}{\partial t} + U\frac{\partial}{\partial x}\right)\frac{\partial \psi}{\partial y} - U'\frac{\partial \psi}{\partial x}\right]_-^+ = 0,$$

and $\partial/\partial t + U\partial/\partial x = 0$ in the inviscid limit. Accordingly, since U' is zero above and non-zero below the interface, we must have

$$D = 0. \tag{7}$$

Hence, there can be no disturbance in the region $0 < y < h$ and, from (6),

$$C = -\mathrm{e}^{\alpha h}(\mathrm{e}^{-\mathrm{i}\alpha kh} + B\,\mathrm{e}^{\mathrm{i}\alpha kh}). \tag{8}$$

In this inviscid limit, B remains arbitrary, but C is known once B is. In order to determine B and C uniquely, a viscous boundary condition must additionally be met.

We shall not attempt to solve the full viscous problem here: rather, a heuristic approach is used which leads to results that are surprisingly successful. Given that the inviscid solution yields no disturbance in $0 < y < h$ and so satisfies the viscous no-slip condition at $y = 0$, we merely suppose that the full viscous solution is likewise zero, or virtually zero, in this region and we match this with the inviscid solution by applying the additional boundary condition that $\partial\psi/\partial y = 0$ at the interface $y = h$. This procedure implicitly assumes that any viscous contribution to the flow disturbance at $y = h$, arising from the wall region, is negligible: for large R, this is likely to be so. Support for this hypothesis is given by figure 3 of I, which shows that there is virtually no disturbance below about $y = 4$. The imposition of this new boundary condition yields

$$-\mathrm{i}k\,\mathrm{e}^{-\mathrm{i}\alpha kh} + \mathrm{i}kB\,\mathrm{e}^{\mathrm{i}\alpha kh} - C\,\mathrm{e}^{-\alpha h} = 0 \tag{9}$$

which combines with (8) to give

$$B = \mathrm{e}^{-2\mathrm{i}\alpha kh}\left(\frac{\mathrm{i}k-1}{\mathrm{i}k+1}\right), \quad C = \mathrm{e}^{\alpha h}\,\mathrm{e}^{-\mathrm{i}\alpha kh}\left(\frac{-2\mathrm{i}k}{\mathrm{i}k+1}\right). \tag{10}$$

In terms of modulus and phase, these are, on using (3),

$$\left.\begin{aligned} |B| &= 1, \quad \mathrm{ph}\,B = \pi - 2\theta - 2\alpha h\tan\theta, \\ |C| &= 2\,\mathrm{e}^{\alpha h}\sin\theta, \quad \mathrm{ph}\,C = -\tfrac{1}{2}\pi - \theta - \alpha h\tan\theta, \end{aligned}\right\} \tag{11}$$

which may be compared with the precise results of I shown in figure 1 (*a*) once a suitable value is assigned to h, which measures the boundary-layer thickness.

In appropriate dimensionless units, the Blasius momentum thickness δ^* is 1.72 and the 'boundary-layer thickness' is 5.04 according to I (p. 42). It turns out that a near 'best fit' is obtained on choosing h to lie about midway between these values: the value $h = 3.44 = 2\delta^*$ is here chosen for illustration and is consistent with figure 3 of I. Results (11) are plotted in figure 2 (*a*, *b*) for this h and for $\alpha = 0.179$ as in figure 1 (*a*).

It is evident that, despite the crude model used, many features of the precise

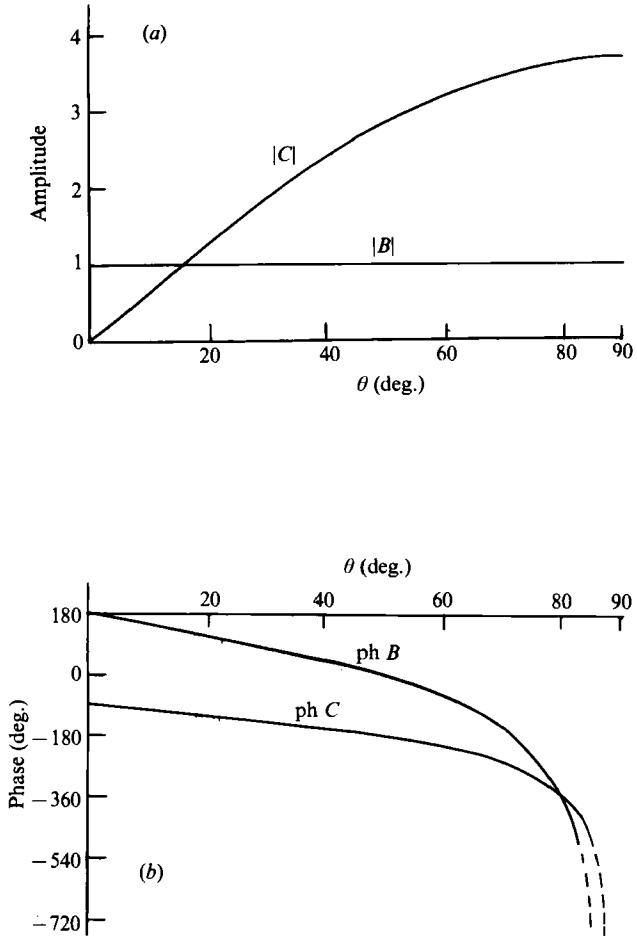

FIGURE 2. Approximate estimates (11) of (*a*) magnitudes and (*b*) phases of the complex amplitudes B and C at $\alpha = 0.179$ with $h = 3.44$.

results shown in figure 1 (*a*) are successfully captured. The greatest shortcoming is in $|B|$, which remains equal to unity for all θ rather than gradually decreasing from unity. That agreement is least good for the largest values of θ is what one would expect: both the viscous damping and the viscous shear stress across the interface are greatest for such modes. The growth of $|C|$ is quite well modelled, but not its decay back to zero at large θ, which is presumably a viscous effect. The increasingly rapid phase variation of both B and C is well represented. The left-hand end points are 180° and 90° for ph (B) and ph(C) according to the model; 180° and 99° according to I. The crossing point where ph (B) = ph (C) is at −360° for all choices of h, according to (11), and the corresponding value of θ is just under 80° when $h = 3.44$. These estimates agree remarkably well with figure 1 (*a*).

3. The jet profile

Grosch & Salwen's jet profile may be similarly modelled. If the profile (4) is extended into $y < 0$ by reflection in the x-axis, and if a new reference frame travelling in the x-direction with speed 1 is adopted, then the resultant flow resembles a symmetric jet travelling from right to left. Now, inviscid disturbances symmetric

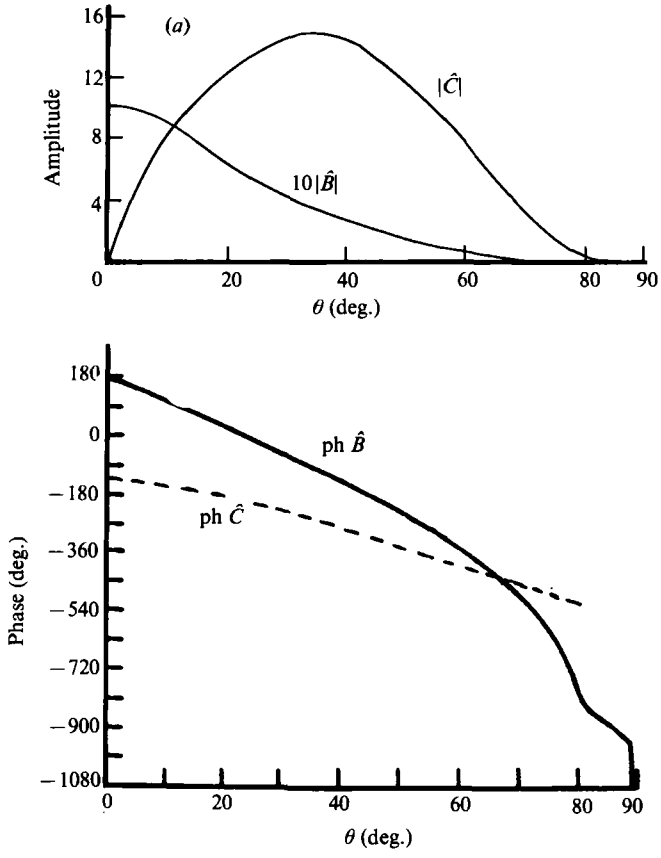

FIGURE 3. Grosch & Salwen's results for the jet profile at $\alpha = 1$ and $R = 50$, rescaled according to the transformation (12).

about the line $y = 0$ are dynamically equivalent to those just studied for the model boundary layer; furthermore, Grosch & Salwen found that symmetric and antisymmetric modes gave nearly identical results. However, to take into account the reversed flow direction, it is necessary to make the transformations

$$x \to -x, \quad v \to \psi^*,$$

where the asterisk denotes complex conjugate. That is to say, it is the coefficient of $\exp[i\alpha(x+ky)]$ that must be normalized to unity in order to remain consistent with (5). Accordingly, the coefficients of the terms in $\exp[i\alpha(x-ky)]$ and $\exp[-\alpha y+i\alpha x]$ are respectively redefined as

$$\hat{B} = \frac{1}{B^*}, \quad \hat{C} = \frac{C^*}{B^*}, \tag{12}$$

where B and C are as in I.

It is immediately seen that Grosch & Salwen's normalization for the jet, which instead took the coefficient of $\exp[i\alpha(x-ky)]$ as unity, will not yield results resembling those for the boundary layer. For this, the rescaling (12) is required. This accounts for the major qualitative differences between figures 1(*a*) and 1(*b*). The rescaling may be done, rather approximately, from enlargements of figure 1(*b*): more detailed plots would require access to the original numerical data.

Figure 3 shows, roughly, these rescaled data, and it certainly more closely resembles figure 1(*a*). $|\hat{B}|$ decreases uniformly from 1 to 0 as θ increases from 0 to 90°,

while $|\hat{C}|$ rises from 0 at $\theta = 0$ to a maximum of around 15 near 35°, and then decreases to zero again.

In order to compare these data with the model, values must be assigned to α and h in (11). For the data of figure 1 (*b*), $\alpha = 1.0$ and the Reynolds number is $R = 50$. The previous choice of $h = 3.44$ suggests

$$|\hat{C}| = 62.4 \sin\theta,$$

which is rather larger than the computed results and, as before, shows no falling off to zero at larger θ. The lower value $h = 2.8$ gives rather better agreement for $|\hat{C}|$ in the range $20° < \Theta < 30°$, but an h-value larger than this is better for $0° < \theta < 20°$.

The rescaled computations give ph $\hat{B} = 180°$ and ph $\hat{C}$ (= ph B − ph C − 360°) = −135° at $\theta = 0$, whereas the model gives ph $\hat{B} = 180°$ and ph $\hat{C} = -90°$. (A much smaller disagreement in ph C at $\theta = 0$ was noted earlier for the boundary layer). The crossing point where ph $\hat{B}$ = ph $\hat{C}$ is at −360° for the model and occurs at around $\theta = 54°$ when $h = 2.8$. The actual crossing point is at a value of θ closer to 65°, with ph $\hat{B}$ = ph $\hat{C}$ at around −400°.

Although there is rough agreement between the model and the now-rescaled computations for the jet, this agreement is far less good than for the boundary layer. This is certainly due to the different Reynolds numbers, 580 for the Blasius flow and just 50 for the jet.

4. Discussion

The initial reason for undertaking this study was the surprising qualitative difference between the computed results of I for the Blasius boundary layer and for the jet. The model problem immediately suggested that the explanation lay in an inconsistent normalization: that is to say, the differences are largely apparent rather than real and more compatible results are achieved by a simple rescaling.

An improved asymptotic model could doubtless be developed to include viscous terms more systematically: see, for example, Drazin & Reid (1981). But for the present purpose of shedding an interpretative light on the computational results of I, this is unnecessary. The present rather crude model suffices to show that the wavelike and evanescent components of a continuous-spectrum disturbance are related in such a way as to give *virtually no disturbance within the shear-layer zone*. A remarkably low level of disturbance in the shear layer is confirmed for special cases described in I.

There remains the question of why the disturbance level is so low in the shear-layer region for these continuous-spectrum modes. The main explanation seems to be that the associated pressure perturbation is very small (zero in the inviscid limit) because $c_r = U_\infty$. Within the free stream, it is only viscous stresses that gradually reduce the disturbance amplitude while the disturbance is convected along with the free-stream speed. In contrast, within the shear layer, convective processes rapidly distort any initial disturbance, producing small vertical scales by tilting of fluid lines in a manner previously described by many, from Kelvin (1887) onwards.

As all inviscid two-dimensional disturbances are vorticity-preserving, the intensity of velocity fluctuations must decay as the vertical scale of sheared disturbances decreases. Also, viscosity will preferentially damp such small-scaled disturbances. In the absence of imposed pressure fluctuations, it is therefore natural that persistent disturbances within the shear layer are weak; for both inviscid shearing and viscous dissipation act to eliminate them. This process is exemplified in recent and ongoing

work by Criminale & Drazin (1990) and W. O. Criminale, F. I. P. Smith & B. Long (in preparation), who discuss the inviscid temporal evolution of more general localized disturbances in various model piecewise-linear shear flows.

This work was undertaken during a brief visit to the University of Washington, supported by the USAF Window on Science Program. Discussions with Professor W. O. Criminale are gratefully acknowledged.

REFERENCES

CRAIK, A. D. D. 1985 *Wave Interactions and Fluid Flows*. Cambridge University Press.

CRIMINALE, W. O. & DRAZIN, P. G. 1990 The evolution of linearized perturbations of parallel flows. *Stud. Appl. Maths* **83**, 123–157.

DRAZIN, P. G. & REID, W. H. 1981 *Hydrodynamic Stability*. Cambridge University Press.

GROSCH, C. E. & SALWEN, H. 1978 The continuous spectrum of the Orr–Sommerfeld equation. Part 1. The spectrum and the eigenfunctions. *J. Fluid Mech.* **87**, 33–54 (referred to herein as I).

KELVIN, LORD 1887 Stability of fluid motion: rectilinear motion of viscous fluid between two parallel plates. *Phil. Mag.* **24** (5), 188–196.